# Theoretical characterization of the LiSH potential energy surface

**Ramon S. da Silva (ramonshowsa@gmail.com) and Maikel Y. Ballester (maikel.ballester@ufjf.edu.br)**

Universidade Federal de Juiz de Fora, Departamento de Física, CEP 36036-330, Juiz de Fora- MG, Brazil

*Article history:* Received: ; revised:; accepted:. Available online:. DOI:

## Abstract

Electronic structure calculations have been performed to characterize the potential energy surface of the LiSH. For such, molecular properties have been calculated using two different levels of theories: DFT/B3LYP and CASSCF. As results, the obtained equilibrium geometry at CAS(8,13)/VQZ level of theory is $R_{Li-S}$ = 4.0975 $a_0$, $R_{S-H}$ = 2.5502 $a_0$, and θ = 93.37°. The present vibrational harmonic frequencies are in good agreement with those previously reported in the literature. Our results show the overall endothermicity of the Li(²P) + SH(X²Π) → H($^2$S) + LiS(X²Π) to be about 0.508 eV without ZPE corrections at CAS(8,13)/VQZ. Besides, the role of the molecular singlet-triplet transitions, essential for the interpretation of the phosphorescence spectra, is discussed. Overall, the present findings reproduced well the experimental ones and, therefore, can be used as a benchmark for other theoretical and experimental studies.

**Keywords:** DFT, Potential energy surface, Dipole moment, Oscillator strength, Radiative lifetime

*Corresponding author. E-mail: ramonshowsa@gmail.com

QUARKS: Brazilian Electronic Journal of Physics, Chemistry and Material Science
journal homepage: https://periodicos.ufjf.br/index.php/quarks
e-ISSN: 2674-9688
| Vol 4 | | No. 1 | | 2022 |

## 1. Introduction

Hydrosulphide compounds have been used in both experimental and theoretical studies, including biological systems [1], molecular dynamics [2], astrochemistry [3], and spectroscopy [4,5]. In particular, molecular properties of the MSH species (M = Li, Na, K, Be, Mg, and Ca) were investigated by Magnusson [6], Pappas [7], and Bucchino *et al.* [8], showing that these structures have a M-S-H angle in about 90º.

The most accurate values obtained for the Li-S and S-H bond lengths are 4.0553 and 2.5360 $a_0$, respectively [5]. Recently, we carried out *ab initio* calculations at the multireference configuration interaction (MRCI) level of theory to examine the Li-S interactions [9]. The equilibrium distance ($R_e$), vibrational harmonic frequency ($\omega_e$), and dissociation energy ($D_0$) for the ground $X^2\Pi$ were calculated to be 4.0948 $a_0$, 572 $cm^{-1}$, and 3.2470 eV, respectively. It can be seen that our $R_e$(Li-S) is comparable to the value reported by Khadri *et al.* [5] for the triatom LiSH.

It should be noted that the previous knowledge of the Li-S interactions is desirable for the study of lithium-sulfur batteries, so important to the development of clean energies [10]. In this scenario, at least two works examined the performance of the LiSH molecule in Li-S batteries [11,12]. According to Islam *et al*., Li-S battery is a good candidate for energy storage devices due to its low cost [12].

At equilibrium geometry, the singlet ground ($S_0$) valence configuration of LiSH is represented as follows [5]:

$$\Psi[X^1A'] = 1\sigma^2 2\sigma^2 1\pi^4 3\sigma^2 4\sigma^2 5\sigma^2 2\pi^4 6\sigma^2 \quad (1)$$

Its corresponding binding energy was estimated by Pappas [7] to be $D_0$(Li-SH) = 7.24 eV at the molecular orbital linear combination of atomic orbital self-consistent field (MO-LCAO-SCF) level of theory. It suggests that the Li(²P) + SH(X²Π) → LiSH($X^1A'$) reaction forms a global minimum with a deep potential well and long lifetimes. Yet, the correct dissociation limit is given by Li(²P) + SH(X²Π) instead of Li(²S) + SH(X²Π) as pointed out in Ref. [5].

The photodissociation of LiSH yields SH(X²Π) formation which, from the astrochemical point of view, deserves considerable attention [13,14]. The total energy using MP2 calculations is -405.75788 $E_h$ at equilibrium geometry R(Li-S) = 4.0534 $a_0$, R(S-H) = 2.5322 $a_0$, and α(Li-S-H) = 91.4 Degrees [6]. Besides, vertical excitation energies for the low-lying states ¹A'', ³A'', ¹A', and ³A' were studied at MRCI/VQZ level of theory [5]. There are no geometric parameters such as bond lengths and vibrational harmonic frequencies reported in the literature for these states, except the vertical transition energies.

The singlet-triplet (S-T) transitions are recognized as being spin-forbidden (ΔS = 2) [15]. The UV absorption ³A''←$X^1A'$ spectrum was predicted in the wavelength region λ ≈ 312 nm [5]. However, no transition parameters such as oscillator strengths and radiative lifetimes were computed for the LiSH. Therefore, we can conclude from the previous paragraphs that our knowledge of the LiSH species is limited. Besides, it is not clear the reaction Li + SH → LiS +

QUARKS: Brazilian Electronic Journal of Physics, Chemistry and Material Science
journal homepage: https://periodicos.ufjf.br/index.php/quarks
e-ISSN: 2674-9688
| Vol 4 | | No. 1 | | 2022 |

H (or LiH + S) is whether exothermic or endothermic. Even already observed in laboratory experiments [16], we can extend these statements to several metal hydrosulfide species like NaSH, MgSH, and CaSH. The reactions between Li atoms and SH are still far from being understood. So, the main goal of this research can be divided into two parts: 1) to characterize the ground and low-lying singlet and triplet excited states of LiSH, including their transitions; 2) to explore the reaction mechanism and energetics of the Li + SH → LiS + H (and LiH + S) through theoretical chemistry calculations.

This paper is divided into three sections. Section 2 gives a brief overview of how the quantum-chemistry calculations were done. The third section is dedicated to presenting the obtained results. A comparison with the theoretical and experimental data is also included to evaluate our findings. In this section, we present a study on the Li + SH reaction, including reliable structures of the reactants, products, and intermediates as well as their energies. The last section is addressed to the final remarks.

## 2. Computational Methods

All electronic structure calculations have been performed using the ORCA quantum chemistry package [17]. We conducted our research as follows: Firstly, the ground electronic state geometry for the triatomic species was optimized under $C_s$ symmetry and compared with available results in the literature. As the next step, potential energy curves were calculated to obtain the $D_0$(Li-SH) values. After these processes, transition properties were computed. At last, the Li + SH reaction was energetically investigated. For such, molecular fragments LiS, LiH, and SH are requested.

To examine the ground state of the chosen species, we employed the density functional theory (DFT) which combines relatively low cost of the calculations and accuracy. For this, the Becke three parameter Lee–Yang–Parr exchange–correlation functional (B3LYP) [18] has been used in combination with the following basis sets: 6-311++G(d,p), Ahlrichs' TZVP [19], Ahlrichs' QZVP [19], and the correlation consistent basis set cc-pVTZ (VTZ) and cc-pVQZ (VQZ) [20]. B3LYP functional is generally faster than most post Hartree-Fock methods and usually yields trustworthy results for small molecules. In the present calculations, we also utilized the scalar relativistic Douglas-Kroll-Hess (DKH) Hamiltonian and relativistically contracted versions of the Karlsruhe basis set (DKH-def2-QZVP) [19].

The multiconfigurational character of the LiSH was investigated using the complete active space self-consistent field (CASSCF) approach as implemented in the ORCA program [17]. In this context, it is possible to distribute a particular number of electrons (active electrons) in a certain number of orbitals (active orbitals). The active space must be carefully selected since influences the molecular properties calculations. In general, the reference space can be represented by CAS(*m*,*n*), where *m* and *n* are the number of active electrons and active orbitals, respectively.

For LiSH, the large active space was built with *3s*, *3p* atomic orbitals (AOs) of the sulfur atom, *2s*, *3s* AOs of the lithium atom, and *1s* atomic orbital of the hydrogen atom. That is, 13 valence electrons were distributed into 8 molecular orbitals (MOs), being denoted as CAS(8,13). The two smallest active spaces were also tested in our exploratory calculations:

QUARKS: Brazilian Electronic Journal of Physics, Chemistry and Material Science
journal homepage:
https://periodicos.ufjf.br/index.php/quarks
e-ISSN: 2674-9688
| Vol 4 | | No. 1 | | 2022 |

CAS(6,6) and CAS(8,8). However, these reference spaces did not prove to be satisfactory for the excited states, including a correct behavior of the asymptotic limits.

The diatomic fragments that compose the reactants/products analyzed have been optimized using the same level of theory as described above. For SH radical, we adopted the reference space given by CAS(7,12), where 7 valence electrons were distributed into 12 molecular orbitals. For Li compounds, LiS and LiH, we used the active spaces CAS(9,8) and CAS(4,9), respectively. Similar active spaces were earlier used in other works [9,21,22].

As a next step, vertical transition energies from the ground state and the oscillator strengths (*f*) have been calculated. To know, the oscillator strength is proportional to the square of the transition moment according to the expression [17]

$$f = frac23\left|\langle\Psi_j\left|er\right|\Psi_i\rangle\right|^2\Delta E, \qquad (2)$$

where ΔE represents the transition energy taken from the ground electronic state. The radiative lifetimes are determined in this work from the relationship [17]

$$\tau = frac1.499\Delta E^2 f \qquad (3)$$

with ΔE in units of $cm^{-1}$.

## 3. Results and Discussions

### 3. 1 Calculated properties of the singlet ground state

Table 1: Geometry optimization for the ground singlet state of LiSH($X^1A'$)

| Method | $R_{Li\text{-}S}/a_0$ | $R_{S\text{-}H}/a_0$ | θ/degree | $\omega_1/cm^{-1}$ | $\omega_2/cm^{-1}$ | $\omega_3/cm^{-1}$ | $\mu_e$/D |
|---|---|---|---|---|---|---|---|
| B3LYP/6-311++G(d,p) | 4.0611 | 2.5546 | 94.31 | 382 | 570 | 2637 | 6.9986 |
| B3LYP/TZVP | 4.1357 | 2.5566 | 96.45 | 404 | 548 | 2633 | 7.3205 |
| B3LYP/QZVP | 4.0593 | 2.5413 | 94.59 | 393 | 571 | 2653 | 6.8236 |
| B3LYP/ DKH-def2-QZVP | 4.0589 | 2.5181 | 94.46 | 399 | 570 | 2619 | 6.8227 |
| B3LYP/VTZ | 4.0576 | 2.5479 | 94.49 | 391 | 570 | 2648 | 6.7067 |
| B3LYP/VQZ | 4.0554 | 2.5433 | 94.53 | 389 | 572 | 2650 | 6.8070 |
| CAS(6,6)/QZVP | 4.0838 | 2.5290 | 94.95 | 414 | 586 | 2724 | 7.2667 |
| CAS(8,8)/QZVP | 4.0656 | 2.5283 | 94.01 | 414 | 594 | 2712 | 7.1609 |
| CAS(8,13)/6-311++G(d,p) | 4.0744 | 2.5660 | 92.96 | 403 | 590 | 2611 | 7.2181 |
| CAS(8,13)/VTZ | 4.1020 | 2.5587 | 95.33 | 394 | 575 | 2623 | 7.0513 |
| CAS(8,13)/VQZ | 4.0975 | 2.5502 | 93.37 | 395 | 574 | 2644 | 7.1638 |
| Exp. [4] | 4.0553 | 2.5567 | 93.0 | - | - | - | - |
| Theo. [5] | 4.0553 | 2.5360 | 93.8 | 372 | 578 | 2571 | 7.03 |
| Theo. [6] | 4.0534 | 2.5322 | 91.4 | - | - | - | - |
| Theo. [7] | 4.1536 | 2.5227 | 97.2 | - | - | - | - |
| Theo. [8] | 4.0912 | 2.5435 | 92.8 | 417 | 566 | 2610 | 7.37 |

We start this discussion by analyzing the obtained molecular properties of the LiSH($X^1A'$). In general, the experimental ground geometry $R_{Li-S}$ = 4.0553 $a_0$, $R_{S-H}$ = 2.5567 $a_0$, and θ = 93° [4] was well reproduced by the present calculations. Table 1 shows our results for the optimized geometry considering the theoretical methods described in Sec. 2. For comparisons, other available data found in the literature have been included. The DFT B3LYP/6-311++G(d,p) calculations provide a ground geometry that differs by 0.01 $a_0$ and 1.3° from the experimental $R_{Li-S}$ and θ. From this table, the worst results are identified for the DFT B3LYP/TZVP when compared with [4] and [5]. Similar geometries are shown for the B3LYP in the VTZ and VQZ basis sets. The inclusion of relativistic effects through DKH-def2-QZVP basis set did not improve our results, where the experimental S-H bond length was underestimated by ~0.03 $a_0$.

The agreement between the CASSCF results and experimental data is fairly good. As can be seen in Table 1, the reference spaces CAS(6,6) and CAS (8,8) provide good predictions for the global minimum of LiSH, however, when the vibrational frequencies and dipole moments are analyzed one can observe disagreement with other results. On the other hand, the active space formed by CAS(8,13) is almost optimum. For example, the optimized CAS(8,13)/6-311++G(d,p) structure ($R_{Li-S}$ = 4.0744 $a_0$, $R_{S-H}$ = 2.5660 $a_0$, and θ = 92.96°) compares well with the MRCI results from Khadri *et al.* [5]. The older theoretical calculations reported by Pappas [7] considerably differ from the present findings. In particular, the CAS(8,13)/VQZ optimized Li-S bond of 4.0975 $a_0$ is too close to the $R_{Li-S}$ = 4.0948 $a_0$ found in [9]. The coupled-cluster results employing the VTZ basis set [8] appear to be in line with our theoretical data. The ground geometry is shown in Fig. 1.

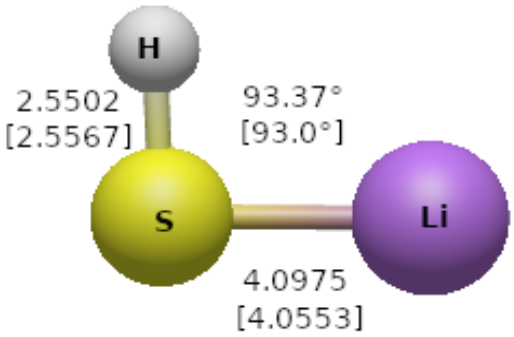


Figure 1: Ball and stick representation of the ground geometry calculated at CAS(8,13)/VQZ level of theory. Distances are in $a_0$ and angles in Degrees. For comparison, the experimental results from [4] are included in brackets.

Considering both DFT and CASSCF methods, we obtain harmonic vibrational frequencies in the range of $\omega_1$ = 382-414 $cm^{-1}$, $\omega_2$ = 548-594 $cm^{-1}$, and $\omega_3$ = 2,611-2,724 $cm^{-1}$. The LiSH bending frequency is represented by $\omega_1$ and the symmetric and antisymmetric frequencies are given by $\omega_2$ and $\omega_3$, respectively. At least two groups [5,8] have calculated these values. Our best estimate is given by CASSCF calculations using the CAS(8,13) associated with Dunning's basis sets VTZ and VQZ. It should be noted that the major discrepancies are shown for $\omega_3$ (SH). In this case, the present CAS(8,13)/VQZ value differs by 2.8% from Ref. [5] and 1.3% from Ref. [8]. To the best of our knowledge, there are no experimental measurements to compare with the present findings. The vibrational spectrum of ground state was studied up to

3,521 $cm^{-1}$ above the minimum by Khadri and coworkers. Taking into account the CAS(8,13)/VQZ level theory, we compute the energies of the vibrational levels (0,0,0), (0,1,0), (0,0,1), and (1,0,0) to be 1806, 2201, 2380, and 4450 $cm^{-1}$, respectively, in good agreement with [5]. Páleníková and coworkers [43] used an active space comparable to our CAS(8,13) to compute molecular properties of the systems $H_2O$ and $H_2S$. Considering the accuracy of their predictions and the present results, we believe that the reference space CAS(8,13) can provide reliable data for the LiSH species.

It is interesting to compare the ground structures of the LiOH and LiSH. Its chalcogenide alkali hydroxide (LiOH) has linear structure given by R(Li-O) = 2.9823 $a_0$, R(O-H) = 1.7913 $a_0$, and θ = 180.0° at coupled-cluster level of theory [23]. Strictly speaking, this value of Li-O bond distance underestimates in 0.246 $a_0$ the results from the ground state of LiO [24]. The corresponding LiOH vibrational frequencies are predicted to be $\omega_1$ = 925 $cm^{-1}$, $\omega_2$ = 319 $cm^{-1}$, and $\omega_3$ = 3,833 $cm^{-1}$. Therefore, the LiOH and LiSH present different structures being the first one linear and the last having a T-shaped form concerning their corresponding minimum geometries. The vibrational energy difference ΔE[(0,1,0) – (0,0,0)] is 317 $cm^{-1}$ for the LiOH and 395 $cm^{-1}$ for the LiSH, with other vibrational modes presenting considerable discrepancies. There are no significant differences in the R(S-H) distance of the species LiSH, NaSH, MgSH, CaSH, and SrSH [4]. The present values of θ(Li-S-H) ~93.0° are close to that reported for the NaSH [4].

In this work, we investigated the electronic properties relative to the ground LiSH species. Table 1 also lists the numerical values of dipole moment calculated at geometry equilibrium ($\mu_e$). The MRCI result available in Ref. [5] is 7.03 D, which differs from our CASSCF calculations by about 0.1881 D (6-311++G(d,p)), 0.0213 D (VTZ), and 0.1338 D (VQZ). All DFT calculations show a dipole moment smaller than 7.0 D, except that calculated at B3LYP/TZVP (7.3205 D). There is no experimental $\mu_e$ available in the literature to compare with our findings. So, we can conclude that the dipole moment for the ground state must be close to 7.0 D, which differs by about 2.25 D from the LiOH in the vibrational state (0,0,0) [25].

As can be seen, this work have shown that CAS(8,13)/6-311++G(d,p) improve the results if compared with experimental ones and the results found in references [5] and [7]. Potential energy curves (PECs) at CAS(8,13)/6-311++G(d,p) for three states of LiSH correlating with the two lowest dissociation asymptotes as a function of Li–S bond length are shown in Fig. 2. In this plot, the R(S-H) distance was fixed at 2.5660 $a_0$ and the bond angle at 92.96°. The bent $X^1A'$ states become the lowest $X^1\Sigma^+$ state, correlating with the second dissociation channel $Li(^2P)$ + $SH(X^2\Pi)$ at large values of R(Li-S). The first dissociation channel $Li(^2S)$ + $SH(X^2\Pi)$ is located 1.8341 eV below the second channel. This value is in good concordance with the MRCI result of 1.85 eV reported by Khadri and coworkers [5]. The $^1\Pi$ and $^3\Pi$ PECs cross the $^1\Sigma^+$ curve around R(Li-S) = 7.0 $a_0$, indicating a predissociation mechanism. The crossing between these states can affect the molecular spectra of the LiSH. In this context, we believe that the spin-orbit coupling (SOC) has an important role, however, SOC calculations will not addressed in this present paper.

The LiSH → $Li(^2P)$ + $SH(X^2\Pi)$ reaction was used to estimate the lower limit to the dissociation energy, $D_e$, for the ground electronic state. That is, the $D_e(X^1A')$ value has been calculated from the energy difference between its geometry equilibrium CAS(8,13)/6-311++G(d,p) ($R_{Li-S}$ = 4.0744 $a_0$, $R_{S-H}$ = 2.5660 $a_0$, and θ = 92.96°) and the dissociation path $Li(^2P)$ + $SH(X^2\Pi)$ with parameters $R_{Li-S}$ = 20.0 $a_0$, $R_{S-H}$ = 2.5660 $a_0$, and θ = 92.96° (see Fig.

2). Our predictions point out for the value of 4.4127 eV. Correcting this value for the zero-point energy (ZPE) of LiSH [0.2234 eV] and SH [0.1639 eV], we can derive $D_e(X^1A') = 4.3532$ eV.

This value deviate in about 2.90 eV from the theoretical one (7.24 eV) reported by Pappas [7]. The ground $D_e$(LiOH) energy calculated from the dissociation channel LiOH → Li + OH was determined to be 4.5098 eV [26]. Thus, we can conclude that the $D_e$(LiOH) and $D_e$(LiSH) are close, however, the $D_e$(LiOH) must be slightly larger than $D_e$(LiSH).

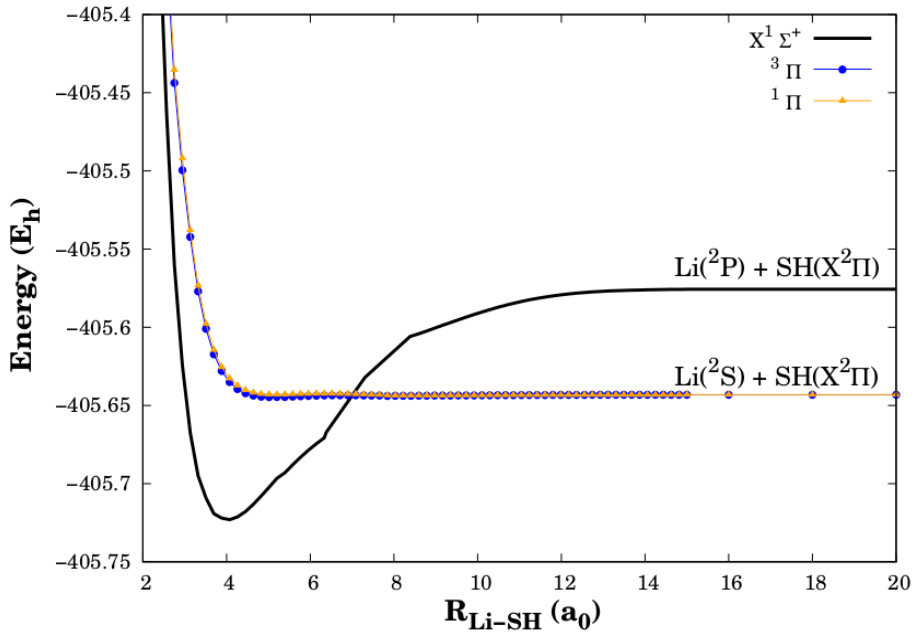


Figure 2: CASSCF PESs collinear cuts of low-lying electronic states of the LiSH for the Li-SH asymptotes.

A previous understanding of the hyperfine structure is desirable in the interpretation of measurements recorded through Electron paramagnetic resonance (EPR) experiments [27]. From this, interactions between the nuclear electric quadrupole moment, $eQ$, with the electric-field gradient, $eq$, can be represented by [28, 29]

$$H_Q = frace^2Qq4I(2I-1)[3I_Z^2 - I^2 + \eta(I_X^2 - I_Y^2)] \quad (4)$$

where the spin angular momentum, ***I,*** has a magnitude of $[I(I+1)]^{1/2}\hbar$; I assume the values of 3/2 for the $^7$Li and $^{33}$S isotopes; for the deuterium, $^2$H, I equals the unity. $\eta$ is dimensionless, being defined as [17]

$$\eta = |fracV_{XX} - V_{YY}V_{ZZ}| \quad (5)$$

where, for instance, $V_{XX}$ is equal to $eq_{xx}$. The parameter $\eta$ is often calculated in the range of 0 and 1. The obtained CAS(8,13)/6-311++G(d,p) results found in the present work are $eQ_{Li}$ = -0.0040 barn, $eQ_S$ = -0.0550 barn, and $eQ_H$ = 0.0029 barn for the nuclei $^7$Li, $^{33}$S, and $^2$H, respectively. These values are in agreement with experimental measurements reported by Stone [30] of $eQ_{Li}$ = -0.0400(3) barn, $eQ_S$ = -0.0678(13) barn, and $eQ_H$ = 0.00286(2) barn. The calculated nuclear quadrupole coupling (NQC) $e^2q_{ZZ}Q_{Li}$ was estimated to be 0.028 MHz associated with$\eta$= 0.497. For sulfur atom, we have $e^2q_{ZZ}Q_S$ = -27.658 MHz and $\eta$= 0.059.

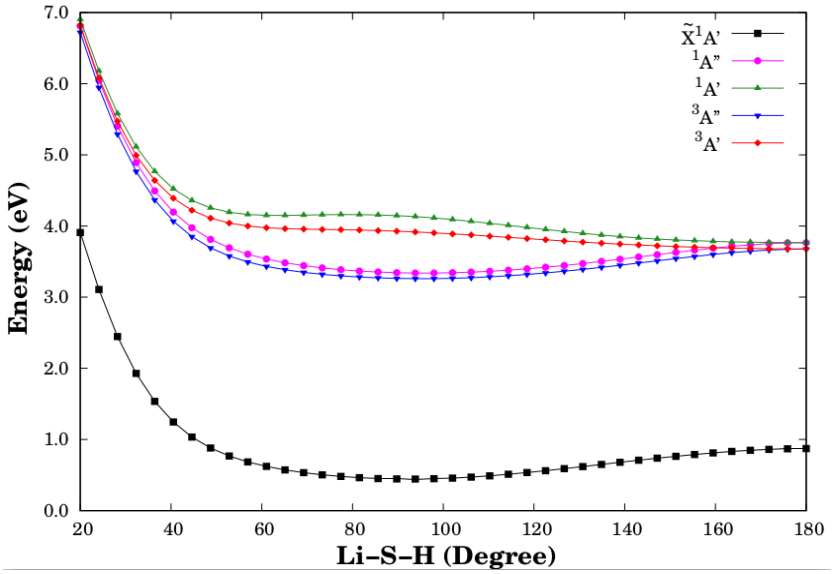


Figure 3: Potential energy curves for the ground singlet and excited states at CAS(8,13)/6-311++G(d,p) level of theory.

At last, the rotational constants $A_e$, $B_e$, and $C_e$ that compose the rotational spectrum have been computed at CAS(8,13)/6-311++G(d,p) [CAS(8,13)/VQZ] level of theory. The present rotational constants are $A_e$ = 285,758 [285,795] MHz, $B_e$ = 18,974 [18,680] MHz, and $C_e$ = 17,792 [17,534] MHz, in agreement with experimental data ($A_0$ = 293,283 MHz, $B_0$ = 18,959 MHz, and $C_0$ = 17,687 MHz) of Janczyk and Ziurys [4]. Our predictions differ by only 1% from the theoretical data of Khadri et al. [5].

### 3. 2 Excited states of LiSH: Vertical energies and transition properties

A potential energy scan was performed to examine the angle dependence of the total energy with the optimized Li-S and S-H bond lengths fixed. The calculated results at CAS(8,13)/cc-pVQZ level of theory are plotted in Fig. 2. These potential energy curves are smooth for the entire range of θ, having a similar shape to those shown by Khadri *et al.* [5]. We identified two excited states with singlet spin multiplicity ($^1A''$ and $^1A'$) and two others with triplet spin multiplicity ($^3A''$ and $^3A'$). The $^1A''$ and $^1A'$ states are henceforth named $S_1$ and $S_2$, while the triplet states are henceforth named $T_1$ and $T_2$. According to Minaev and coworkers [31], the excited $T_1$ state is energetically located below $S_1$ in some systems like HCN, $O_3$, $H_2O$, and $H_2S$. The present findings are in concordance with their statements [$E(^3A'') < E(^1A'')$], showing that HOMO-LUMO exchange integrals play an important role in the calculations of these species. Table 2 shows vertical transition energies (ΔE) for the low-lying singlet and triplet states calculated from the ground state geometry in both CASSCF and DFT levels of theories. The oscillator strengths (f) and radiative lifetimes for the spin-allowed transitions S→S have been estimated at TDDFT B3LYP. We call the attention that the oscillator strengths for the spin-forbidden transitions S-T are not available in the ORCA program.

The geometry optimization of the excited $^1A''$ state computed at CAS(8,13)/6-311++G(d,p) level of theory shows that it has a similar structure to the ground state. We obtained the following molecular parameters: $R_{Li-S}$ = 4.9730 $a_0$, $R_{S-H}$ = 2.5794 $a_0$, and θ = 93.58°. Its corresponding dipole moment at equilibrium is 0.9254 D. One can find vertical transition energy

(ΔE) from the ground state of 3.621 eV (342.4 nm), in agreement with the MRCI value of 3.737 eV [5]. Besides, the present DFT B3LYP/6-311++G(d,p) calculations provide energy of 3.409 eV (363.7 nm) and oscillator strength 0.0465 while the obtained B3LYP/VQZ value is 3.634 eV (341.2 nm) and oscillator strength 0.0438. The $S_1 \rightarrow S_0$ transitions are stronger and can be observed in discharge experiments. Our $^1A''$ radiative lifetime is 39.75 ns at B3LYP/VQZ and 42.62 ns at B3LYP/6-311++G(d,p), suggesting that the transition originated from these states occurs readily.

The difference energy $\Delta E(S_2 - S_0)$ = 4.105 eV has been estimated for the CAS(8,13)/6-311++G(d,p) level of theory, which differs by about 0.2 eV from the DFT results. Our value is in line with the CASSCF value of 4.125 eV [5], however, underestimates in 0.26 eV the MRCI prediction reported in the same reference. In this case, the present DFT calculations lead to *f* equals 1.83 x $10^{-4}$ [6-311++G(d,p)] and 1.01 x $10^{-4}$ [cc-pVQZ], showing that the $S_2 \rightarrow S_0$ transitions are weaker than the $S_1 \rightarrow S_0$. With these findings, we calculate radiative lifetimes on the microsecond scale.

The first excited triplet state, $T_1$, has the following structure $R_{Li-S}$ = 4.9708 $a_0$, $R_{S-H}$ = 2.5642 $a_0$, θ = 95.83°, and dipole moment of 4.1905 D at CAS(8,13)/6-311++G(d,p) level of theory. As displayed in Table 2, the energy separation $\Delta E(T_1 - S_0)$ has been predicted to be 3.417 eV at CAS(8,13) and 3.409 eV at DFT/B3LYP. In both cases, we use the 6-311++G(d,p) basis set. These values are somewhat different from the Ref. [5]. Only for comparison, the energy separation between the ground triplet state and the first excited state of LiCH species is calculated at V5Z basis set to be 0.6857 eV [32]. Besides, we note that the CASSCF results of Khadri *et al.* [5] show curves in which the triplet state $T_1$ is below the lowest singlet state $S_1$. Nevertheless, they reported the electronic excitation energy for the $T_1$ state of 3.685 eV, i.e., this value is 0.214 eV above the $S_1$ state, in contradiction with their figure and the present findings. The same situation is displayed for the $T_2$ and $S_2$ excited states.

Table 2: Vertical energies calculated from the ground singlet state geometry of LiSH. The oscillator strengths and radiative lifetimes for the singlet-singlet transitions are also listed.

| State | Method | ΔE (eV) | *f* | τ (ns) |
|---|---|---|---|---|
| **$S_1$** | CAS(8,13)/6-311++G(d,p) | 3.621 | - | - |
| | B3LYP/VQZ | 3.634 | 0.043890 | 39.75 |
| | B3LYP/6-311++G(d,p) | 3.409 | 0.046518 | 42.62 |
| **$S_2$** | CAS(8,13)/6-311++G(d,p) | 4.105 | - | - |
| | B3LYP/VQZ | 4.331 | 0.000183 | $6.71 \times 10^3$ |
| | B3LYP/6-311++G(d,p) | 4.305 | 0.000101 | $12.31 \times 10^3$ |
| **$T_1$** | CAS(8,13)/6-311++G(d,p) | 3.417 | - | - |

| | | | | |
|---|---|---|---|---|
| | B3LYP/VQZ | 3.429 | - | - |
| | B3LYP/6-311++G(d,p) | 3.409 | - | - |
| $T_2$ | CAS(8,13)/6-311++G(d,p) | 4.071 | - | - |
| | B3LYP/VQZ | 4.367 | - | - |
| | B3LYP/6-311++G(d,p) | 4.238 | - | - |

We highlight that the T → S transitions are spin-forbidden and have an important role in phosphorescence studies as discussed in [31,41]. For the LiSH species, we have that the $S_0$ → $S_2$ absorption can occur induced by UV light. In turn, the singlet state $S_2$ can decay to triplet $T_2$ through the nonradiative process of intersystem crossing (ISC) [41]. The $T_2$ → $T_1$ transition it is possible in terms of internal conversion (IC). Following this pathway, it is possible to obtain the $T_1$ → $S_0$ phosphorescence. Of course, this suggestion still needs to be evidenced in an experiment.

### 3. 3 Products in the Li + SH reaction

In the present section we will discuss the formation of the LiSH from the channel Li + SH and their probable products. Therefore, to characterize the relative energies of the reactants, the intermediate, and products, geometry optimizations have been performed from CASSCF and DFT methods at different basis sets. The resulting energies are listed in Table 3.

We calculate the following energy separation of the lithium atom ΔE(²P - ²S) equals to 1.8438 eV for the CAS/6-311++G(d,p) in good agreement with the experimental value of 1.8477 eV [33]. The B3LYP provides splittings of 1.8231 [6-311++G(d,p)], 1.6628 [VTZ], and 1.9624 eV [VQZ], showing higher differences in comparison with the experimental one. For the sulfur atom, the ΔE($^1$D - $^3$P) energy separation was estimated to be 1.1738 eV at CAS/6-311++G(d,p), 1.3243 eV at CAS/VTZ, and 1.3913 eV CAS/VQZ. In this case, the better ΔE value is determined at CAS/6-311++G(d,p) when compared with the experimental data of 1.1455 eV [34]. For comparison, Swope, Lee, and Schaefer reported theoretical ΔE values close to 1.4397 eV [35], which differs by about 0.30 eV from the experimental measurement [34].

Table 3: Energies (in hartrees) for LiSH and its fragments

| Species | CAS/6-311++G(d,p) | CAS/VTZ | CAS/VQZ | B3LYP/6-311++G(d,p) | B3LYP/VTZ | B3LYP/VQZ |
|---|---|---|---|---|---|---|
| H(²S) | - | -0.49980 | -0.49994 | - | - | - |
| Li(²S) | -7.43243 | -7.43298 | -7.43405 | -7.48097 | -7.48165 | -7.48186 |
| Li(²P) | -7.36467 | -7.36522 | -7.36637 | -7.41397 | -7.42054 | -7.40974 |
| S($^3$P) | -397.51258 | -397.51190 | -397.51888 | -398.07210 | -398.07773 | - |
| S($^1$D) | -397.46944 | -397.46323 | -397.46775 | - | - | - |

| | | | | | | |
|---|---|---|---|---|---|---|
| SH($X^2\Pi$) | -398.20190 | -398.21231 | -398.21759 | -398.70837 | -398.71556 | -398.71994 |
| LiS($X^2\Pi$) | -405.04437 | -405.06536 | -405.06535 | -405.66924 | -405.67567 | -405.68011 |
| LiH($X^1\Sigma^+$) | -8.03005 | -8.03270 | -8.03388 | -8.07236 | -8.07321 | -8.07405 |
| LiSH($X^1A'$) | -405.73790 | -405.77648 | -405.76837 | -406.31226 | -406.31989 | -406.32499 |

For $C_{2v}$ symmetry, we found that the ground state of LiS, LiH, and SH fragments are $X^2\Pi$, $X^1\Sigma^+$, and $X^2\Pi$, respectively. In the next paragraphs, we will analyze their characteristics regarding spectroscopic parameters. Molecular properties for the diatomic fragments in their ground states have been studied using the CASSCF and DFT/B3LYP level of theories in combination with 6-311++G(d,p), VTZ, and VQZ basis sets. These results are collected in Table 4. Evaluating the DFT/B3LYP energies, it is possible to observe that, for the systems of interest, the correlation consistent basis sets VTZ and VQZ present a monotonic convergence in energetic properties with increasing basis set size, however, it is not always true as discussed by Wang and Wilson [36-37], see also references therein.

For the LiS($X^2\Pi$), the harmonic vibrational frequency is calculated in the range of 560-605 $cm^{-1}$, in qualitative accord with experimental [38] and theoretical [9] data. At B3LYP/6-311++G(d,p) [B3LYP/VTZ] {B3LYP/VQZ} level of theory the bond distance is 4.0729 [4.0662] {4.0627} $a_0$, consistent with the experimental measurement of 4.0623 $a_0$. The dipole moment has been estimated in the range of 6.76 to 7.25 D, indicating which $\mu_e$(LiS) is sensitive concerning the level of theory/basis set. Our best estimate is given by the CASSCF calculations in comparison with the theoretical value of 7.2261 D [9]. Kudo, Yokoyama and Wu [39] reported a ZPE value of 0.03469 eV at MP2/6-31+G* level of theory. This value of ZPE compares well with our calculations.

Table 4: Theoretical equilibrium structure for the diatomic fragments. Other theoretical and experimental data were extracted from [9,21,38,38].

| Species | | CAS/6-311++G(d,p) | CAS/VTZ | CAS/VQZ | B3LYP/6-311++G(d,p) | B3LYP/VTZ | B3LYP/VQZ | Exp. | Theo. |
|---|---|---|---|---|---|---|---|---|---|
| LiS($X^2\Pi$) | $R_e/a_0$ | 4.0491 | 4.0933 | 4.0742 | 4.0729 | 4.0662 | 4.0627 | 4.0623 | 4.0948 |
| | $\omega_e/cm^{-1}$ | 605 | 588 | 594 | 560 | 562 | 565 | 580 | 572 |
| | $\mu_e$/D | 7.2487 | 7.1036 | 7.2064 | 7.0551 | 6.7697 | 6.8586 | - | 7.2261 |
| | ZPE/eV | 0.03754 | 0.03647 | 0.03683 | 0.03472 | 0.03488 | 0.03506 | 0.03596 | 0.03546 |
| | | | | | | | | | |
| SH($X^2\Pi$) | $R_e/a_0$ | 2.5591 | 2.5650 | 2.5600 | 2.5574 | 2.5509 | 2.5464 | 2.5333 | 2.5416 |
| | $\omega_e/cm^{-1}$ | 2,644 | 2,611 | 2,617 | 2,650 | 2,657 | 2,658 | 2,696 | 2,704 |
| | $\mu_e$/D | 1.0641 | 0.9139 | 0.8623 | 1.0293 | 0.8462 | 0.7984 | - | 0.758 |
| | ZPE/eV | 0.16394 | 0.16187 | 0.16224 | 0.16433 | 0.16476 | 0.16480 | 0.16440 | 0.16763 |
| | | | | | | | | | |
| LiH($X^1\Sigma^+$) | $R_e/a_0$ | 3.0205 | 3.0415 | 3.0435 | 3.0133 | 3.0079 | 3.0065 | 3.015 | 3.060 |
| | $\omega_e/cm^{-1}$ | 1,407 | 1,381 | 1,358 | 1,412 | 1,416 | 1,407 | 1,405 | 1,374 |
| | $\mu_e$/D | 5.8029 | 5.8779 | 5.8814 | 5.7249 | 5.6892 | 5.7034 | 5.88 | 5.89 |
| | ZPE/eV | 0.08723 | 0.08561 | 0.08421 | 0.08758 | 0.08784 | 0.08724 | 0.08709 | 0.08518 |

For the SH($X^2\Pi$), Resende and Ornellas [21] reported the following values os spectroscopic constants $R_e$ = 2.5416 $a_0$, $\omega_e$ = 2,704 $cm^{-1}$, and $\mu_e$ = 0.758 D. These values correlate favorably with the present B3LYP/VQZ. Notwithstanding the lack of agreement, the CASSCF calculations provide harmonic vibrational frequencies about 80 $cm^{-1}$ below the experimental one of 2,696 $cm^{-1}$, see Ref. [21] and references therein. The present DFT calculations predict bond lengths of ~2.55 $a_0$, which by approximately 0.8% from the experimental measurement (2.5333 $a_0$). We obtained the dipole moment within the limits of 0.7984 and 1.0641 D.

Therefore, we consider the present results as reliables.

For the LiH($X^1\Sigma^+$), we determined the following values $R_e$ = 3.0205 $a_0$, $\omega_e$ = 1,407 $cm^{-1}$, and $\mu_e$ = 5.8029 D at CASSCF/6-311++G(d,p). These spectroscopic constants are consistent with the experimental measurements of $R_e$ = 3.015 $a_0$, $\omega_e$ = 1,405 $cm^{-1}$, and $\mu_e$ = 5.88 D [40]. The configuration interaction results reported in Ref. [40] agree well with our CASSCF results. The B3LYP approach reproduces reasonably well the experimental data $R_e$ and $\mu_e$, showing an error of about 0.2% and 3%, respectively. In both cases, the DFT/B3LYP and CASSCF level of theories lead us to trustworthy results. Therefore, we used these data to investigate the Li + SH reaction, including the products of this reaction.

Table 5 lists the DFT and CASSCF relative energies relative to Li($^2$P)+SH($X^2\Pi$) with and without ZPE corrections. The Li atom attacks the S atom of the SH($X^2\Pi$), leading to an intermediate adduct LiSH($X^1A'$). The energy difference between the entrance channel Li($^2$P)+SH($X^2\Pi$) and the intermediate LiSH($X^1A'$) has been estimated to be -4.6621 eV at CAS/6-311++G(d,p). This value is reduced to -4.6025 eV when the corresponding ZPE energies are taken into account. To confirm this result, we carried out calculations by using the CAS/VQZ level of theory. We found a value of -5.0181 eV (without ZPE corrections) in qualitative agreement with the CAS/6-311++G(d,p) result. The difference between these values can be justified, at least in part, by the correlation consistent basis set used (i.e., VQZ) which, according to Dunning [20], systematically recovers the correlation energy. Therefore, the CAS/6-311++G(d,p) may be interpreted as a lower limit to LiSH formation if the Li($^2$P)+SH($X^2\Pi$) reaction is considered a start point.

It should be noted that a comparison of 47 functionals was done by Goerigk and Grimme [44]. These authors showed that the B3LYP functional presented worst predictions when compared with other functionals in the analysis of reaction energies. So reaction energies would be one of the places to be careful about using B3LYP. In this paper, B3LYP calculations were performed just to compare with the CASSCF results. Also, the theoretical calculations carried out by Lee and Wright [26] showed that the intermediate LiOH has an energy formation, in magnitude, of 4.61 eV without ZPE corrections (or 4.50 eV with ZPE corrections) relative to Li + OH collisions. This result is comparable with our CASSCF calculations, showing the reliability of the present findings.

The present findings calculated at CAS/6-311++G(d,p), without ZPE corrections, shows that the reaction Li($^2$P) + SH($X^2\Pi$) → H($^2$S) + LiS($X^2\Pi$) is weakly endothermic (0.6057 eV). The relative energy including ZPE corrections is determined to be 0.4793 eV, which is ~0.13 eV below the result not including such a correction. These values correlate favorably well with the CAS/VQZ calculations (with and without ZPE corrections). The calculated DFT results combining the B3LYP functional and the 6-311++G(d,p) basis set point out that the mentioned reaction is exothermic by 1.4041 eV, not including any ZPE correction. Even providing structural properties for the diatomic fragments comparable to experimental ones, the choice of a density functional that is suitable for a determined problem of interest it is not

straightforward. For example, it was shown the poor performance of the B3LYP functional in computing an accurate energy separation of the lithium atom. It suggests that the values found must to be sensitive to the choice of functional. DFT calculations tend to converge more quickly concerning *ab initio* methods, however, the choice of the optimal functional is still in discussion since several kinds of functionals are available in the literature [42]. We believe that it can be a possible cause of this discrepancy.

A similar issue occurs when we analyze the reaction Li(²P) + SH(X²Π) → S($^3$P) + LiH(X$^1\Sigma^+$). The CASSCF results reveal that this reaction is endothermic by 0.6514 eV (or 0.5747 eV with ZPE corrections). On the contrary, the B3LYP/6-311++G(d,p) provides an energy gap of -0.6786 eV, against the results from CASSCF calculations. Besides, the reaction Li(²P) + SH(X²Π) → S($^1$D) + LiH(X$^1\Sigma^+$) is predicted to be highly endothermic at CASSCF level of theory. No DFT result was computed in this case. The present findings may be used as a benchmark for future theoretical and experimental studies involving Hydrosulphide species.

Table 5: DFT and CASSCF relative energies relative to Li(²P)+SH(X²Π).

| No. | intermediate/products | ΔE/eV | | |
|---|---|---|---|---|
| | | CAS/6-311++G(d,p) | CAS/VQZ | B3LYP/6-311++G(d,p) |
| **1** | LiSH(X$^1$A') | -4.6621 (-4.6025) | -5.0181 (-4.9563) | -5.1680 (-5.1097) |
| **2** | H($^2$S) + LiS(X²Π) | 0.6057 (0.4793) | 0.5080 (0.3825) | -1.4041 (-1.2745) |
| **3** | S($^3$P) + LiH(X$^1\Sigma^+$) | 0.6514 (0.5747) | 0.8489 (0.7708) | -0.6786 (-0.6019) |
| **4** | S($^1$D) + LiH(X$^1\Sigma^+$) | 1.8253 (1.7486) | 2.3633 (2.2852) | - |

## 4. Final Remarks

In this work, a detailed CASSCF and DFT study is presented to investigate LiSH Hydrosulphide species. The total and ZPE corrected relative energies were calculated, showing that the reaction Li(²P) + SH(X²Π) → H($^2$S) + LiS(X²Π) is weakly endothermic by 0.6057 eV. The considered ground state of LiSH is a low-spin with $^1$A' symmetry. At CAS(8,13)/VQZ level of theory, we compute the following LiSH(X$^1$A') structure: $R_{Li\text{-}S}$ = 4.0975 $a_0$, $R_{S\text{-}H}$ = 2.5502 $a_0$, and θ = 93.37°. The calculated dissociation energy was estimated to be $D_e$(Li-SH) = 4.3532 eV. Its corresponding rotational constants have been obtained in line with experimental values. We can conclude that the absorption spectra from these species are in the ultraviolet region. A plausible mechanism for a $T_1 \rightarrow S_0$ photophosphorescence was here introduced.

## Acknowledgments

This study was financed by the Coordenação de Aperfeiçoamento de Pessoal de Nível Superior (CAPES) - Finance Code 001. Financial support from CNPQ is also aknowledged.

## References

[1] Czyzewski, B.K., Wang, D.N. *Nature*, 2012, **483**, 494. https://doi.org/10.1038/nature10881.

[2] Ballester, M.Y., Guerrero, Y.O., Garrido, J.D. *International Journal of Quantum Chemistry*, 2008, **108**, 1705. http://dx.doi.org/10.1002/qua.21591

[3] Vidal, T.H., Loison, J.C., Jaziri, A.Y., Ruaud, M., Gratier, P., Wakelam, V. *Monthly Notices of the Royal Astronomical Society*, 2017, **469**, 435. https://doi.org/10.1093/mnras/stx828

[4] Janczyk, A., Ziurys, L.M. *Chemical Physics Letters*, 2002, **365**, 514. https://doi.org/10.1016/S0009-2614(02)01504-X

[5] Khadri, F., Zaidi, A., Lahmar, S., Ben Lakhdar, Z., Rosmus, P., Hochlaf, M. *Molecular Physics*, 2007, **105**, 2315. http://dx.doi.org/10.1080/00268970701581465

[6] Magnusson, E. *The Journal of Physical Chemistry A*, 2001, **105**, 3881. http://dx.doi.org/10.1021/jp003621n

[7] Pappas, J.A. *Journal of the American Chemical Society*, 1978, **100**, 6023. http://dx.doi.org/10.1021/ja00487a008

[8] Bucchino, M.P., Sheridan, P.M., Young, J.P., Binns, M.K.L., Ewing, D.W., Ziurys, L.M. *The Journal of chemical physics*, 2013, **139**, 214307. https://doi.org/10.1063/1.4834656

[9] Da Silva, R.S., Ballester, M.Y. *Chemical Physics*, 2020, ***539***, 110935. https://doi.org/10.1016/j.chemphys.2020.110935

[10] Liu, J., Qian, T., Wang, M., Liu, X., Xu, N., You, Y., & Yan, C. *Nano letters*, 2017, **17**, 5064. http://doi.org/10.1021/acs.nanolett.7b02332

[11] Rice, J.E., Gujarati, T.P., Motta, M., Takeshita, T.Y., Lee, E., Latone, J. A., & Garcia, J. M. *The Journal of Chemical Physics*, 2021, **154**, 134115. https://doi.org/10.1063/5.0044068

[12] Islam, M.M., *et al. Physical Chemistry Chemical Physics,* 2015, **17**, 3383. https://doi.org/10.1039/C4CP04532G

[13] Kłos, J., Lique, F., Alexander, M.H. *Chemical Physics Letters*, 2009, **476**, 135. https://doi.org/10.1016/j.cplett.2009.04.063

[14] Yamamura, I., Kawaguchi, K., Ridgway, S.T. *The Astrophysical Journal Letters*, 1999, **528**, L33. https://doi.org/10.1086/312420

[15] Minaev, B., Tunell, I., Salek, P., Loboda, O., Vahtras, O., Ågren, H. *Molecular Physics*, 2004, **102**, 1391. https://doi.org/10.1080/00268970410001668435

[16] Bucchino, M. P., Sheridan, P. M., Young, J. P., Binns, M. K. L., Ewing, D. W., Ziurys, L. M. *The Journal of chemical physics*, 2013, **139**, 214307. http://dx.doi.org/10.1063/1.4834656

[17] Neese, F. *Wiley Interdisciplinary Reviews: Computational Molecular Science*, 2021, **2**, 73. https://doi.org/10.1002/wcms.81; Cai, Z. L., Hirsch, G., Buenker, R. J. *Chemical physics letters*, 1996, *255*, 350. https://doi.org/10.1016/0009-2614(96)00395-8.

[18] Beck, A.D. *The Journal of Chemical Physics*, 1993, **98**, 5648. https://doi.org/10.1063/1.464913

[19] Weigend, F., Ahlrichs, R. *Physical Chemistry Chemical Physics*, 2005, **7**, 3297. https://doi.org/10.1039/B508541A

[20] Woon, D.E., Dunning Jr, T.H. *The Journal of chemical physics*, 1993, **98**, 1358. https://doi.org/10.1063/1.464303

[21] Resende, S.M., Ornellas, F.R. *The Journal of chemical physics*, 2001, **115**, 2178. http://dx.doi.org/10.1063/1.1381577

[22] Ma, J., Li, S., Li, W. *Journal of computational chemistry*, 2006, **27**, 39. https://doi.org/10.1002/jcc.20319

[23] Koput, J. *The Journal of Chemical Physics*, 2013, **138**, 234301. http://dx.doi.org/10.1063/1.4810864

[24] da Silva, R. S., Ballester, M. Y. *Chemical Physics*, 2021, **545**, 111123. https://doi.org/10.1016/j.chemphys.2021.111123

[25] Higgins, K. J., Freund, S. M., Klemperer, W., Apponi, A. J., Ziurys, L. M. *The Journal of Chemical Physics*, 2004, **121**, 11715. https://doi.org/10.1063/1.1814631

[26] Lee, E. P. F.; Wright, T. G. *Chemical Physics Letters*, 2002, **352**, 385. https://doi.org/10.1016/S0009-2614(01)01494-4

[27] Schweiger, A. *Applied Magnetic Resonance*, 1993, **5**, 229. https://doi.org/10.1007/BF03162524

[28] Minaev, B., Loboda, O., Vahtras, O., Ågren, H., Bilan, E. *Spectrochimica Acta Part A: Molecular and Biomolecular Spectroscopy*, 2002, **58**, 1039. https://doi.org/10.1016/S1386-1425(01)00580-7

[29] Puzzarini, C., Stanton, J. F., Gauss, J. *International Reviews in Physical Chemistry*, 2010, **29**, 273. https://doi.org/10.1080/01442351003643401

[30] Stone, N. J. *Atomic Data and Nuclear Data Tables*, 2016, **111**, 1.

[31] Minaev, B., Tunell, I., Salek, P., Loboda, O., Vahtras, O., Ågren, H. *Molecular Physics*, 2004, **102**, 1391. https://doi.org/10.1080/00268970410001668435

[32] Montgomery, J. M., Alexander, E., Mazziotti, D. A. *The Journal of Physical Chemistry A*, 2020, **124**, 9562. https://doi.org/10.1021/acs.jpca.0c07134

[33] Radziemski, L. J., Engleman Jr, R., Brault, J. W. *Physical Review A*, 1995, **52**, 4462. https://doi.org/10.1103/PhysRevA.52.4462

[34] Moore, C. E. Atomic energy levels, Vol. 1 (*National Standard Reference Data Series, National Bureau of Standards, Washington, 1971)*

[35] Swope, W. C., Lee, Y. P., Schaefer III, H. F. *The Journal of Chemical Physics*, 1979, **70**, 947. http://dx.doi.org/10.1063/1.437484

[36] Wang, N. X., Wilson, A. K. *The Journal of Physical Chemistry A*, 2003, **107**, 6720. https://doi.org/10.1021/jp0353791

[37] Wang, N. X., & Wilson, A. K. *The Journal of Physical Chemistry A*, 2005, **109**, 7187. https://doi.org/10.1021/jp045622b

[38] Brewster, M. A., Ziurys, L. M. *Chemical physics letters*, 2001, **349**, 249. https://doi.org/10.1016/S0009-2614(01)01202-7

[39] Kudo, H., Yokoyama, K., Wu, C. H. *The Journal of chemical physics*, 1994, **101**, 4190. https://doi.org/10.1063/1.467469

[40] Brown, R. E., Shull, H. *International Journal of Quantum Chemistry*, 1968, **2**, 663. https://doi.org/10.1002/qua.560020507
[41] Mai, S., Marquetand, P., González, L. *International Journal of Quantum Chemistry*, 2015, **115**, 1231. https://doi.org/10.1002/qua.24891

[42] Mardirossian, N., Head-Gordon, M. *Molecular Physics*, 2017, **115**, 2315. https://doi.org/10.1080/00268976.2017.1333644

[43] Páleníková, J., Kraus, M., Neogrády, P., Kellö, V., Urban, M. *Molecular Physics*, 2008, **106**, 2333. https://doi.org/10.1080/00268970802454786

[44] Goerigk, L., Grimme, S. *Physical Chemistry Chemical Physics*, 2011, **13**, 6670. https://doi.org/10.1039/C0C